

**THE SYNTHESIS, VIBRATIONAL SPECTRA, CRYSTAL STRUCTURE AND
THERMAL DECOMPOSITION OF $(\text{N}_2\text{H}_5)_3\text{AlF}_6^\dagger$**

A. Rahten, P. Benkič, A. Jesih

Jožef Stefan Institute, Jamova 39, 1111 Ljubljana, Slovenia

(Received 16.4.1999)

Abstract

$(\text{N}_2\text{H}_5)_3\text{AlF}_6$ has been synthesized by the reaction of $\text{AlF}_3 \cdot 3\text{H}_2\text{O}$ and $\text{N}_2\text{H}_5\text{F}$ in a water solution. N-N stretching bands of the N_2H_5^+ ions appear as medium band at 969 and as strong band at 955 cm^{-1} in infrared and at 965 and 955 cm^{-1} in Raman indicating different environments of the environment sensitive N_2H_5^+ ions. The compound crystallizes in orthorhombic system, space group $\text{P}2_12_12_1$ (No.19), with $a=9.015(2)$ Å, $b=9.191(2)$ Å and $c=10.479(2)$ Å. $(\text{N}_2\text{H}_5)_3\text{AlF}_6$ consists of separated AlF_6^{-3} octahedra, arranged in a distorted f.c.c. fashion. Octahedra are connected through hydrazinium ions and there are two types of strong hydrogen bonds regarding the orientation of $\text{NH}_2\text{-NH}_3^+$ units. $(\text{N}_2\text{H}_5)_3\text{AlF}_6$ decomposes thermally by exothermic decomposition of hydrazinium(+1) ions to yield the mixture of $(\text{NH}_4)_3\text{AlF}_6$ and NH_4AlF_4 at 243 °C. Further decomposition leads to NH_4AlF_4 at 301 °C and $\beta\text{-AlF}_3$ at 460 °C. The final decomposition product is $\alpha\text{-AlF}_3$ at 700°C.

Introduction

Fluoroaluminates decompose on heating to yield AlF_3 at temperatures higher than 460 °C. The course of thermal decomposition depends strongly also on cationic part of fluoroaluminates and on their structures. By the thermal decomposition of fluoroaluminates with different cations like pyridin H^+ and $(\text{CH}_3)_4\text{N}^+$, different new phases of AlF_3 were prepared: $\eta\text{-AlF}_3$ [1], $\kappa\text{-AlF}_3$ [1] and $\theta\text{-AlF}_3$ [1, 2] besides already known and well characterized phases $\alpha\text{-AlF}_3$ and $\beta\text{-AlF}_3$ as well as intermediates in new crystal modifications - $\beta\text{-NH}_4\text{AlF}_4$ [1]. AlF_3 has found wide application as catalyst in

[†]Dedicated to the memory of Prof. Dr. Jože Šiftar

the production of fluorocarbons and its use is grown in the course of seek for CFC alternative materials. The activity of AlF_3 to catalyse reactions depends upon its structure and specific surface area. Fluoroaluminates with hydrazinium(+1) and (+2) cations afford considerable volumes of gaseous products to be evolved during thermal decomposition which allow for large specific surface area of formed solid products. $\text{N}_2\text{H}_6\text{AlF}_5$ [3], $(\text{N}_2\text{H}_5)_2\text{AlF}_5 \cdot \text{H}_2\text{O}$ [4] and $(\text{N}_2\text{H}_5)_2\text{AlF}_5$ [4] were isolated in the past and a very pure AlF_3 was formed as final product of thermal decomposition of $(\text{N}_2\text{H}_5)_2\text{AlF}_5 \cdot \text{H}_2\text{O}$ [4]. The search for different hydrazinium(+1) fluoroaluminates resulted in the synthesis of $(\text{N}_2\text{H}_5)_3\text{AlF}_6$, which is a member of a $(\text{N}_2\text{H}_5)_3\text{MF}_6$ family of compounds, where M stands for V [5], Cr [5], Fe [6], and Ga [7].

Experimental

1. Reagents. N_2H_4 was prepared by the fractional distillation of $\text{N}_2\text{H}_4 \cdot \text{H}_2\text{O}$ (Merck, 80%), over solid NaOH in a nitrogen atmosphere [8]. $\text{N}_2\text{H}_5\text{F}$ was prepared by the reaction of anhydrous N_2H_4 and solid $\text{N}_2\text{H}_6\text{F}_2$ on a water bath. After cooling [9] the $\text{N}_2\text{H}_5\text{F}$ was filtered and dried. $\text{AlF}_3 \cdot 3\text{H}_2\text{O}$ (Aldrich, 97 %), was used as received.

2. Synthesis. $\text{AlF}_3 \cdot 3\text{H}_2\text{O}$ was dissolved in 4.3 % water solution of $\text{N}_2\text{H}_5\text{F}$ (mole ratio $\text{AlF}_3 \cdot 3\text{H}_2\text{O} : \text{N}_2\text{H}_5\text{F} = 1 : 3.15$). New compound $(\text{N}_2\text{H}_5)_3\text{AlF}_6$ was isolated by slow evaporation and crystallization at room temperature. The product was kept in a desiccator with silicagel.

3. Analyses. Hydrazine content was determined by potentiometric titration with potassium iodate [10] and the content of ammonia by Kjeldahl method [11]. For the determination of aluminum and fluorine the new method was developed which utilises alkaline sample total decomposition and subsequent dissolution at $\text{pH} < 3$. Fluorine was determined by ionic selective electrode using reagent for masking aluminum ions [12], and aluminum by substitution titration at $\text{pH}=10$ [13].

Chemical analyses for $(\text{N}_2\text{H}_5)_3\text{AlF}_6$: Observed: % N_2H_4 39.8; %Al 11.2; %F 46.8. Calc.: % N_2H_4 40.04; %Al 11.24; %F 47.47.

4. Thermal analyses. Thermal analyses were done on Mettler thermoanalyser TA-1 in argon atmosphere. 100 mg of sample was decomposing in a 0.9 ml platinum crucible, the reference material was α -Al₂O₃. Measurements were made by measurement head TD-1 in the flow of argon at 5 L/min and heating rate 1 °min⁻¹. In experiments where intermediates were isolated, 250 – 300 mg of sample was used. The temperatures at which thermal effects are recorded depend on the amount of a sample and the same thermal effects correspond to some 15 – 20 °C higher temperatures in case of analyses starting with 300 mg samples compared to analyses started with 100 mg samples.

5. Vibrational spectroscopy. Infrared spectra were recorded on Perkin-Elmer FTIR 1710 spectrometer as Nujol and fluorolube mulls pressed between CsBr and NaCl and as powders pressed between CsBr windows in the range 220 – 4000 cm⁻¹. Raman spectra were recorded on dispersion Raman instrument Renishaw Ramascope, System 1000. As excitation source the 632.8 nm He-Ne laser line or near-infrared semiconductor 782 laser diode line was used. Raman spectra were recorded in the range 100 – 4000 cm⁻¹ using low power excitation line to prevent sample decomposition.

6. Structure determination. Single crystal data were collected on a Rigaku AFC7S diffractometer with graphite monochromated Mo-K_α radiation at a temperature of 23(1) °C using the ω -2 θ scan technique to a maximum 2 θ value of 65.0 °. Scan of $(1.42 + 0.35 \tan \theta)^\circ$ were made at a speed of 8.0 °/min (in ω). The weak reflections ($I < 10.0\sigma(I)$) were rescanned with maximum of 4 scans and the counts were accumulated to ensure good counting statistics. The computer-controlled slits were set to 3.0 mm (horizontal) and 3.0 mm (vertical). Only asymmetric set of data was collected with decay of standards 5.6 %. Further details are given in Table 1.

The structure was solved using direct methodes. After refinement of all non-hydrogen atoms including anisotropic displacement parameters, the positions of hydrogen atoms were located in a difference map and finally refined isotropic without any restrains being applied (Table 2). For better refinement of hydrogen atoms correction for secondary extinction was applied. An empirical psi-absorption correction based on azimuthal scans of several reflections was applied which resulted in

transmission factors ranging from 0.93 to 1.00. All calculations were performed using the teXsan [14] crystallographic software package of Molecular Structure Corporation.

Table 1: Crystal data and structure refinement

Empirical Formula	$\text{N}_6\text{H}_{15}\text{AlF}_6$
Formula Weight	240.13
Wavelength	0.71069 Å
Space Group	$P2_12_12_1$ (No.19)
Lattice Parameters	a = 9.015(2) Å b = 9.191(2) Å c = 10.479(2) Å V = 868.3(2) Å ³
Z value	4
ρ_{calc}	1.837 g/cm ³
$\mu(\text{MoK}\alpha)$	3.06 mm ⁻¹
F_{000}	496.00
Crystal Dimensions	0.24 × 0.24 × 0.40 mm
Number of independent data	1825
Number of observed ($I > 2\sigma_I$)	1484
Number of Variables	179
Refinement	Full-matrix least-squares on F^2
Least Squares Weights	$1/\sigma^2(F_o) = 4F_o^2/\sigma^2(F_o^2)$
p-factor	0.091
Residuals ($I > 2\sigma_I$): R1; wR2	0.076; 0.11
Residuals (all data): R1; wR2	0.079; 0.12
Goodness of Fit Indicator	0.92
Max Shift/Error in Final Cycle	0.00

$$* R1 = \sum ||F_o| - |F_c|| / \sum |F_o|$$

$$wR2 = [\sum (w (F_o^2 - F_c^2)^2) / \sum w(F_o^2)^2]^{1/2}$$

Table 2: Final Positional and Displacement Parameters

Atom	x	y	z	B _{iso} /B _{eq}
Al	0.45623(7)	0.51210(7)	0.54802(7)	0.0123(1)
F1	0.6407(2)	0.4369(2)	0.5317(2)	0.0250(3)
F2	0.4813(2)	0.5336(2)	0.7205(1)	0.0237(3)
F3	0.2719(2)	0.5830(2)	0.5614(2)	0.0246(3)
F4	0.4290(2)	0.4904(2)	0.3774(1)	0.0198(3)
F5	0.3859(2)	0.3301(2)	0.5738(2)	0.0276(3)
F6	0.5281(2)	0.6942(2)	0.5259(2)	0.0226(3)
N1	0.2624(3)	0.2885(3)	0.8026(2)	0.0199(4)
N2	0.1748(3)	0.1599(3)	0.7832(3)	0.0269(5)
N3	0.2422(3)	0.2670(3)	0.2996(2)	0.0214(4)
N4	0.3055(3)	0.1657(3)	0.2105(2)	0.0248(5)
N5	0.5766(3)	0.4822(3)	0.9687(2)	0.0214(4)
N6	0.4934(3)	0.5828(3)	1.0478(2)	0.0233(4)
H1	0.187(8)	0.353(7)	0.826(6)	0.062(6)
H2	0.335(6)	0.261(5)	0.866(5)	0.047(7)
H3	0.298(5)	0.313(5)	0.727(4)	0.026(6)
H4	0.130(7)	0.171(7)	0.704(5)	0.054(6)
H5	0.251(9)	0.091(8)	0.763(6)	0.079(5)
H6	0.203(5)	0.212(4)	0.353(5)	0.029(7)
H7	0.310(8)	0.344(7)	0.328(6)	0.068(5)
H8	0.174(5)	0.305(4)	0.249(4)	0.023(6)
H9	0.329(6)	0.224(5)	0.146(6)	0.049(7)
H10	0.385(4)	0.130(4)	0.252(3)	0.017(6)
H11	0.665(8)	0.504(6)	0.960(6)	0.065(5)
H12	0.550(5)	0.389(4)	0.994(4)	0.027(7)
H13	0.548(4)	0.487(4)	0.890(4)	0.019(6)
H14	0.399(5)	0.550(5)	1.049(4)	0.030(6)
H15	0.489(5)	0.666(5)	1.004(4)	0.025(6)

$$B_{eq} = 8/3 \pi^2 (U_{11}(aa^*)^2 + U_{22}(bb^*)^2 + U_{33}(cc^*)^2 + 2U_{12}(aa^*bb^*)\cos \gamma + 2U_{13}(aa^*cc^*)\cos \beta + 2U_{23}(bb^*cc^*)\cos \alpha)$$

Table 3: Anisotropic Displacement Parameters

Atom	U ₁₁	U ₂₂	U ₃₃	U ₁₂	U ₁₃	U ₂₃
Al	0.0160(3)	0.0160(3)	0.0148(3)	0.0003(2)	0.0007(2)	-0.0005(2)
F1	0.0222(7)	0.0416(8)	0.0310(8)	0.0112(6)	0.0048(6)	0.0097(7)
F2	0.0348(8)	0.0404(9)	0.0147(6)	0.0030(7)	-0.0028(6)	-0.0010(5)
F3	0.0200(7)	0.0405(8)	0.0330(9)	0.0064(6)	-0.0003(6)	-0.0094(7)
F4	0.0287(6)	0.0291(7)	0.0174(6)	-0.0009(7)	-0.0011(5)	-0.0022(5)
F5	0.052(1)	0.0202(7)	0.0328(9)	-0.0086(7)	0.0169(8)	-0.0004(6)
F6	0.0363(9)	0.0205(6)	0.0290(8)	-0.0061(6)	-0.0007(6)	0.0008(5)
N1	0.028(1)	0.0245(9)	0.023(1)	-0.0015(8)	0.0032(9)	0.0008(8)
N2	0.039(1)	0.029(1)	0.033(1)	-0.007(1)	0.005(1)	-0.004(1)
N3	0.031(1)	0.026(1)	0.025(1)	0.0017(9)	-0.0013(9)	0.0007(8)
N4	0.037(1)	0.028(1)	0.029(1)	-0.004(1)	0.009(1)	-0.0014(9)
N5	0.032(1)	0.030(1)	0.0190(9)	-0.0055(9)	-0.0034(7)	0.0042(8)
N6	0.029(1)	0.033(1)	0.027(1)	-0.0065(9)	0.0003(9)	0.0024(9)

Supplemental material is available from authors.

Results and Discussion

1. Vibrational spectra. Partial assignment of $(\text{N}_2\text{H}_5)_3\text{AlF}_6$ vibrational spectra was done by comparison to the spectra of $(\text{N}_2\text{H}_5)_3\text{VF}_6$ [15], $(\text{N}_2\text{H}_5)_3\text{CrF}_6$ [16] and to the spectra of fluoroaluminates [17, 18, 19]. According to primarily the position of the N-N vibration and then the frequencies of the N-H deformation and rockings, N_2H_5^+ compounds have been divided into three groups [15]: where the stretching frequency is between 950 and 980 cm^{-1} , where the N-N vibration is likewise at ca 980 cm^{-1} and where the N-N vibration is between 1000 and 1020 cm^{-1} .

The bands in vibrational spectra of $(\text{N}_2\text{H}_5)_3\text{AlF}_6$ correspond to the spectra of the first group, N-N stretching appears at 955 cm^{-1} with strong band and with medium band at 969 cm^{-1} (Figure 1, Table 4) Two distinct stretching frequencies indicate different environments of the environment sensitive N_2H_5^+ ions in the solid $(\text{N}_2\text{H}_5)_3\text{AlF}_6$. In related compounds corresponding bands appear at 975 and 950 cm^{-1} in the spectra of $(\text{N}_2\text{H}_5)_3\text{CrF}_6$ [16] and at 960 and 949 cm^{-1} in the spectra of $(\text{N}_2\text{H}_5)_3\text{VF}_6$ [15].

Bands which correspond to the N-N stretching appear strong both in Raman and infrared spectra of $(\text{N}_2\text{H}_5)_3\text{AlF}_6$ which is again characteristic of N_2H_5^+ ion [15].

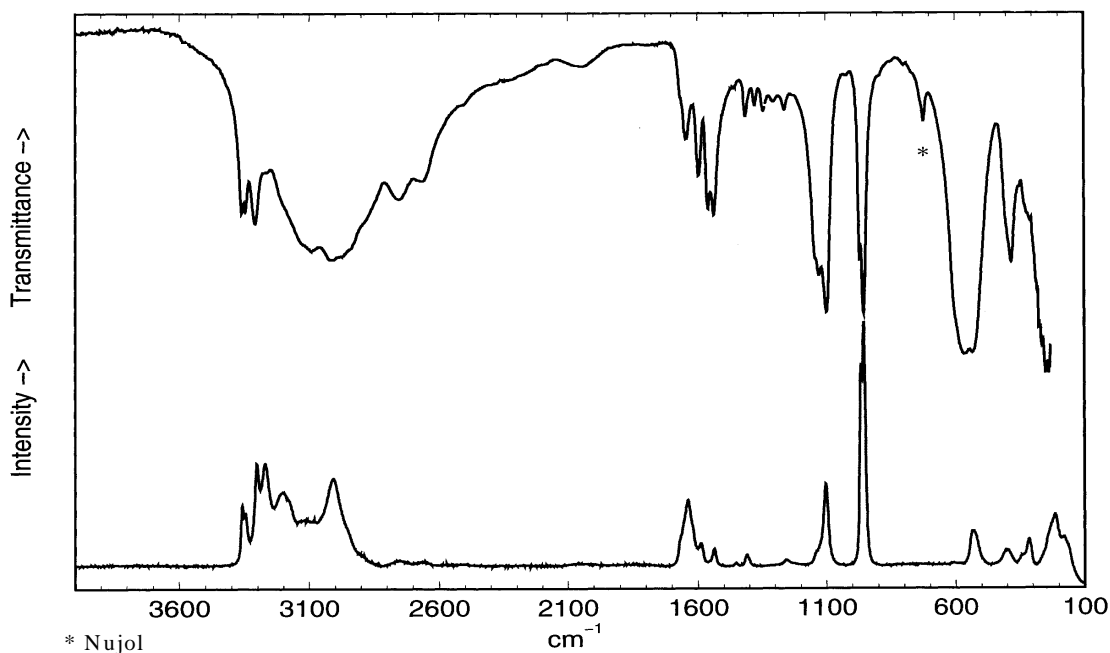


Figure 1: Infrared and Raman spectra of $(\text{N}_2\text{H}_5)_3\text{AlF}_6$.

Table 4: Infrared and Raman spectra of $(\text{N}_2\text{H}_5)_3\text{AlF}_6$ from 4000 to 950 cm^{-1}

<i>IR</i> <i>v/ cm-1</i>	<i>Raman</i> <i>v/cm-1</i>	<i>Assignment</i> *	<i>IR</i> <i>v/ cm-1</i>	<i>Raman</i> <i>v/cm-1</i>	<i>Assignment</i> *
3363 vs	3360 (2.5)	} $(\text{NH}_2)_s$	1595 s	1590 (1)	} $(\text{NH}_3^+)_d$
3350 vs	3348 (2)		1559 s		
3313 vs	3304(4)		1537 s	1538 (2)	
3265 vw	3272 (4)			1453 (1)	} $(\text{NH}_2)_r$
	3199 (3)	1414 w	1410 (1)		
3093 vs	3111 (2)	} $(\text{NH}_3^+)_s$	1306 vw		} $(\text{NH}_3^+)_r$
3009 vs	3008 (4)		1261 vw	1256 (1)	
2755 s	2754 (1)			1128 s	1136 (2)
2667 s	2662 (1)			1098 s	1102 (3.5)
2047 w	2047 (1)	comb. band	969 sho	965 (8)	} $(\text{N-N})_s$
	1667 sho	} $(\text{NH}_2)_d$	955 s	955 (10)	
1641 m	1639 (3)				

Legend: s – strong, m – medium, w – weak, v – very, sho - shoulder.

Raman intensities are given in parentheses.

* s – stretching, d – deformation, r – rocking.

AlF_6^{3-} ion of octahedral symmetry has six fundamental frequencies, two of them are infrared active - ν_3 and ν_4 , three are Raman active, ν_1 , ν_2 and ν_5 , while the ν_6 is inactive.

The bands in vibrational spectra of octahedral AlF_6^{3-} ion (Table 5) are very close to the calculated values [19]. Infrared active frequencies ν_3 and ν_4 which are usually both observed in infrared spectra of fluorometallates appear as strong band at 564 cm^{-1} and as medium band at 383 cm^{-1} . Three Raman active vibrations ν_1 , ν_2 and ν_5 appear at 531, 404 and 315 cm^{-1} . ν_1 also appears in Raman, and the ν_6 frequency was observed in both Raman and infrared due to the departure of AlF_6^{3-} ion from the ideal octahedral symmetry.

Table 5: Infrared and Raman spectrum of $(\text{N}_2\text{H}_5)_3\text{AlF}_6$ below 600 cm^{-1}

<i>IR</i> <i>v/cm⁻¹</i>	<i>R</i> <i>v/cm⁻¹</i>	<i>Assignment</i>
564 vs		ν_3 (F_{1u}) AlF_6^{3-}
535 m	531 (1)	ν_1 (A_{1g}) AlF_6^{3-}
	404 (1)	ν_2 (E_g) AlF_6^{3-}
383 m		ν_4 (F_{1u}) AlF_6^{3-}
309 sho	315 (1)	ν_5 (F_{2g}) AlF_6^{3-}
	215 (2)	ν_6 (F_{2u}) AlF_6^{3-}
	180 (1)	Lattice vibrations

2. Description of the structure. $(\text{N}_2\text{H}_5)_3\text{AlF}_6$ is isostructural with already known compounds $(\text{N}_2\text{H}_5)_3\text{CrF}_6$ [20] and $(\text{N}_2\text{H}_5)_3\text{GaF}_6$ [7]. Some differences arise because of different properties of anions. The structure consists of separated quite regular AlF_6^{3-} octahedra, which are arranged in a distorted f.c.c. fashion (Figure 2). The octahedra are connected through hydrazinium ions, where extensive hydrogen bonding of $\text{N-H}\cdots\text{F}$ type is present (Figure 3).

There are two types of strong hydrogen bonds in sense of orientation of $\text{NH}_2\text{-NH}_3^+$ units. So each hydrogen atom on $-\text{NH}_3$ part of hydrazinium ion (atoms N1, N3 and N5) interacts with different AlF_6^{3-} octahedra in hydrogen bond of $-\text{NH}_2\text{-H}\cdots\text{F}$ type. Hydrogen atoms on N6 atom additionally participate in strong hydrogen bonds of $-\text{NH}\text{-H}\cdots\text{F}$ type with atoms F5 and F3 respectively (Figure 3, Table 6A). In distance limit [21] 3.00 \AA two fluorine atoms around the N4 atom are also found, but in respect with orientation of hydrogen atoms this contact can be more likely considered as weaker bifurcated hydrogen bond between F3 and F6 atoms arising from different AlF_6^{3-} octahedra (Table 6B). In mentioned distance limit no fluorine atoms can be found around N2 atom.

On AlF_6^{3-} unit all fluorine atoms are involved in hydrogen bonding, where each of five fluorine atoms strongly interact with two hydrogen atoms arising from two different N_2H_5^+ units. All strong hydrogen bonds are of $-\text{NH}_2\text{-H}\cdots\text{F}$ type with exception of F5 atom, where one hydrogen bond is of $-\text{NH}\text{-H}\cdots\text{F}$ type. F3 atom participates only in the one strong hydrogen bond of $-\text{NH}\text{-H}\cdots\text{F}$ type (Figure 3, Table 6). In 3.00 \AA distance limit F3 atom is also surrounded with three other nitrogen atoms but positions of hydrogen atoms could only justify weak bifurcated hydrogen bond to N3 and N4 atom arising from same hydrazinium ion and even weaker interactions with N1 (Table 7B). Consequence of considerable weaker hydrogen bonding on F3 atom is probably shorter distance Al-F3 in comparison with other distances in octahedral AlF_6^{3-} (Table 7).

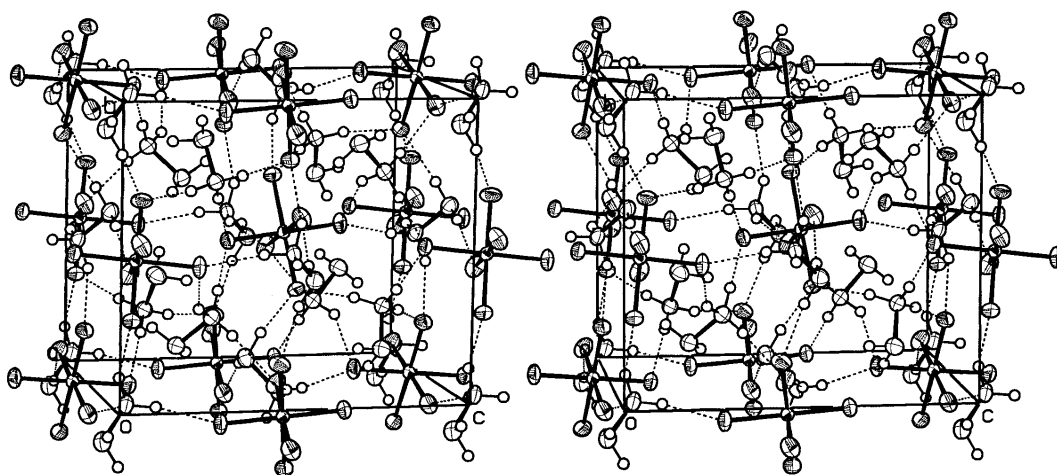


Figure 2: ORTEP [22] stereoview of unit cell packing.

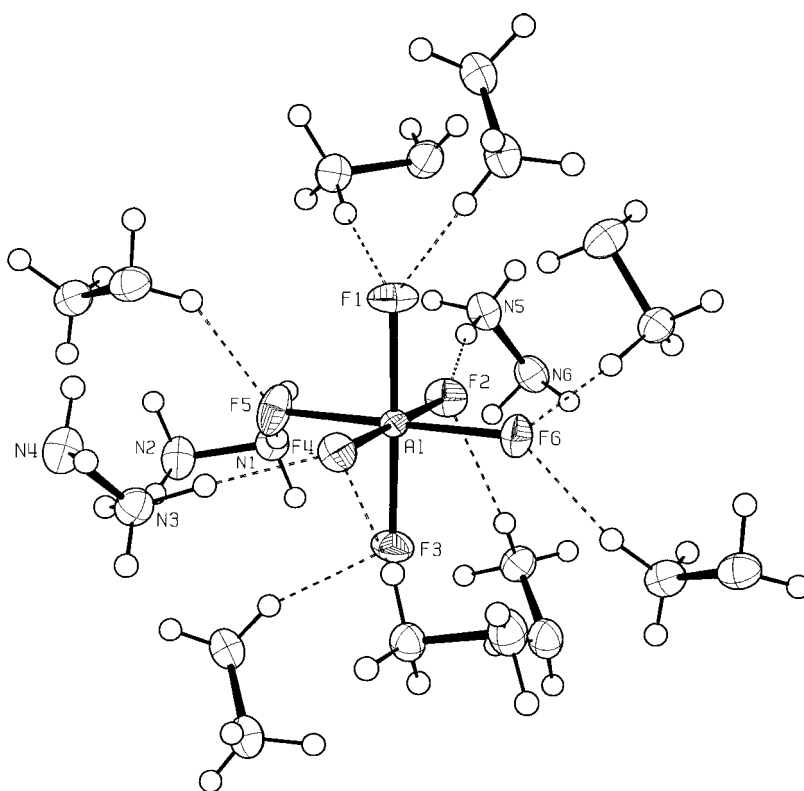


Figure 3: ORTEP view of asymmetric unit (labelled atoms) with NH_2NH_3^+ environment of AlF_6^{3-} anion.

Table 6: Hydrogen Bonds

A) The strongest hydrogen bonds of N–H...F type:

Distances (Å)		Angles (Deg)		Type
F1–N3'	2.734(7)	N3'—H6'...F1	170(4)	–NH ₂ —H...F
F1–N5'	2.736(5)	N5'—H11'...F1	151(6)	–NH ₂ —H...F
F2–N3'	2.846(7)	N3'—H8'...F2	147(3)	–NH ₂ —H...F
F2–N5	2.780(4)	N5—H13...F2	170(3)	–NH ₂ —H...F
F3–N6'	2.839(6)	N6'—H14'...F3	161(4)	–NH—H...F
F4–N1'	2.778(7)	N1'—H1'...F4	167(6)	–NH ₂ —H...F
F4–N3	2.777(7)	N3—H7...F4	177(6)	–NH ₂ —H...F
F5–N1	2.671(5)	N1—H3...F5	170(4)	–NH ₂ —H...F
F5–N6'	2.824(7)	N6'—H15'...F5	144(4)	–NH—H...F
F6–N1'	2.748(7)	N1'—H2'...F6	175(4)	–NH ₂ —H...F
F6–N5'	2.812(4)	N5'—H12'...F6	156(4)	–NH ₂ —H...F

B) Some weaker interactions:

Distances (Å)		Angles (Deg)		Type
F3–N1'	2.974(5)	N1'—H1'...F3	107(4)	–NH ₂ —H...F
F3–N3'	2.854(6)	N3'—H8'...F3	123(3)	–NH ₂ —H...F
F3–N4'	2.874(7)	N4'—H9'...F3	134(5)	–NH—H...F
F6–N4'	2.907(6)	N4'—H9'...F6	133(4)	–NH—H...F
N2–N4'	3.093(5)	N2—H5...N4'	122(6)	–NH—H...N
N4'–N2	3.093(5)	N4'—H10'...N2	105(2)	–NH—H...N
N2–N5'	3.041(7)	N5'—H12'...N2	108(3)	–NH—H...N

' denotes atoms generated with symmetry codes.

It can be concluded, that despite of three crystallographically distinct N₂H₅⁺ units, with respect to the strength of hydrogen bonds, there are only two distinct kinds of hydrazinium ions (Table 7).

Table 7: Interatomic Distances and Angles**Distances (Å):**

<i>Anion AlF₆³⁻</i>			
Al-F1	1.809(3)	Al-F2	1.832(2)
Al-F3	1.791(3)	Al-F4	1.816(2)
Al-F5	1.809(3)	Al-F6	1.809(3)

<i>Cations N₂H₅⁺</i>	
N1-N2	1.436(4)
N3-N4	1.437(5)
N5-N6	1.451(5)

Angles (deg) in anion AlF₆³⁻:

<i>Cis</i>			
F1-Al-F2	91.2(2)	F1-Al-F4	89.4(2)
F1-Al-F5	89.0(2)	F1-Al-F6	90.7(2)
F2-Al-F3	89.9(2)	F2-Al-F5	89.7(2)
F2-Al-F6	89.0(2)	F3-Al-F4	89.5(2)
F3-Al-F5	90.0(2)	F3-Al-F6	90.3(2)
F4-Al-F5	89.9(2)	F4-Al-F6	91.4(2)

<i>Trans</i>	
F1-Al-F3	178.51(9)
F2-Al-F4	179.28(8)
F5-Al-F6	178.72(9)

2. Thermal decomposition. The thermal decomposition of sample starts at 128 °C with endothermic effect which is not accompanied by loss of weight (Figure 4). Similar effect, explained by the melting of sample, was observed at 125 °C during the thermal decomposition of $(\text{N}_2\text{H}_5)_3\text{CrF}_6$ [16] and during the thermal decomposition of $(\text{N}_2\text{H}_5)_3\text{VF}_6$ [23].

The DTA peak at 198 °C corresponds to the strongly exothermic decomposition of hydrazinium(+1) ions. The decomposition is accompanied by weight loss which at 230 °C amounts 30.3 % (Table 8). The analysis of intermediate isolated at 243 °C is: %NH₄ 24.0; %Al 14.9; %F 58.3; Calc. for $(\text{NH}_4)_3\text{AlF}_6$: %NH₄ 27.74; %Al 13.83; %F 58.43; Calc. for NH_4AlF_4 : %NH₄ 14.91; %Al 22.30; %F 62.80. The analysis, x-ray powder data (Table 9) as well as infrared spectra of the intermediate (Figure 5) confirm intermediate isolated at 243 °C being a mixture of $(\text{NH}_4)_3\text{AlF}_6$ and NH_4AlF_4 . Similar thermal behaviour was observed during the thermal decomposition of $(\text{N}_2\text{H}_5)_3\text{CrF}_6$ [16], where at the same experimental conditions $(\text{N}_2\text{H}_5)_3\text{CrF}_6$ decomposed to $(\text{NH}_4)_3\text{CrF}_6$. After the endothermic DTA peak at 257 °C intermediate was isolated at 301 °C. The analysis of intermediate gave: %NH₄ 14.7; %Al 21.3; %F 61.3. The thermal effect is connected to the further decomposition of $(\text{NH}_4)_3\text{AlF}_6$ into NH_4AlF_4 which is the main product at this temperature. The composition has been confirmed also by infrared spectra (Figure 4) [24] which correspond to the infrared spectra of NH_4AlF_4 . NH_4F formed at this stage may cause some hydrolyses to occur on further decomposition, due to its reaction with a quartz wall and H₂O production [25].

NH_4AlF_4 decompose further on and the intermediate isolated at 356 °C has the composition: %NH₄ 10.0; %Al 24.0; %F 61.7 which indicates NH_4AlF_4 decomposed partly. According to the powder diffraction data it may be concluded that hydrolysis products have formed in small quantities too [26, 27].

Intermediate isolated at 460 °C contains mainly $\beta\text{-AlF}_3$, with small quantities of NH₄. Analysis: %NH₄ 0.5-1.3. The final product of the thermal decomposition of $(\text{N}_2\text{H}_5)_3\text{AlF}_6$ isolated at 700 °C is $\alpha\text{-AlF}_3$. Analyses: 65.9% F, Calc. for AlF_3 : 67.87 %. The powder diffraction pattern of the product corresponds to the $\alpha\text{-AlF}_3$.

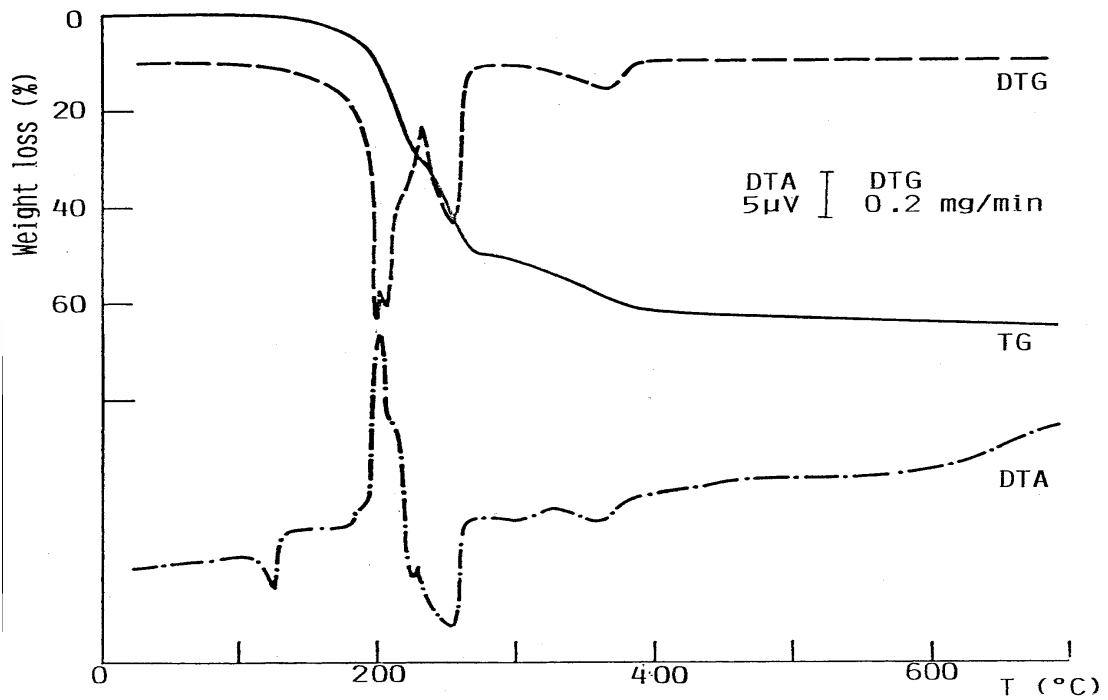


Figure 4: TG, DTG and DTA curves for $(\text{N}_2\text{H}_5)_3\text{AlF}_6$.

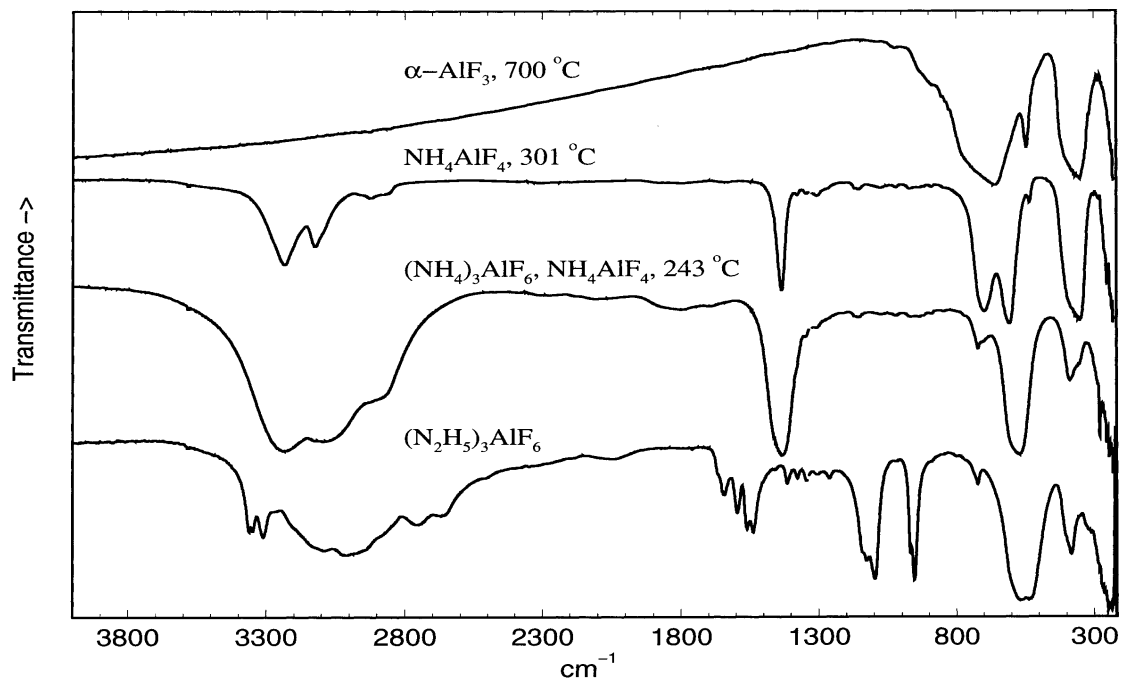


Figure 5: Infrared spectra of $(\text{N}_2\text{H}_5)_3\text{AlF}_6$ and of thermal decomposition products in order of isolation.

Table 8: Thermal behaviour of $(\text{N}_2\text{H}_5)_3\text{AlF}_6$

Temp. (°C)	Intermediate	Weight loss (%)		DTA effects (°C)
		Calc.	Found	
230	$(\text{NH}_4)_3\text{AlF}_6$, NH_4AlF_4		30.3	198 exo
268	NH_4AlF_4	49.61	48.9	257 endo
338	Mostly NH_4AlF_4		54.3	
470	Impure β - AlF_3		63.1	312 endo, 368 endo
690	α - AlF_3	65.03	65.5	

Weight of the sample – 100mg.

Table 9: Powder diffraction data for the intermediates isolated at the thermal decomposition of $(\text{N}_2\text{H}_5)_3\text{AlF}_6$

Intermediate at 243°C		$(\text{NH}_4)_3\text{AlF}_6^a$		Intermediate at 301°C		$\text{NH}_4\text{AlF}_4^b$	
d (Å)	I	d (Å)	I	d (Å)	I	d(Å)	I
6.42	w			6.34	s	6.346	100
5.17	vs	5.15	100				
4.47	s	4.46	55				
3.60	vw			3.59	s	3.585	80
				3.19	w	3.175	10
3.15	s	3.157	45				
2.580	m	2.579	20	3.13	s	3.128	80
				2.54	m	2.534	30
				2.37	m-w	2.364	40
2.232	s	2.233	30	2.24	w	2.234	10
				2.12	w	2.114	15
2.053	w	2.049	4				
1.996	w	1.998	3	1.991	vw	1.984	10
1.826	m-w	1.824	6	1.830	m	1.823	25
				1.797	s-m	1.790	50
1.718	m	1.720	11	1.731	m-w	1.724	15
				1.608	m	1.603	15
1.580	m-w	1.579	5	1.591	m-w	1.585	7
				1.560	m	1.557	20
1.514	w	1.510	4				
1.491	w	1.489	2				
				1.453	vw	1.456	7
1.414	m	1.412	4				
		1.363	2	1.372	vw	1.368	10
		1.347	1			1.347	3
		1.290	2				
1.252	vw	1.2514	2	1.281	vw	1.279	15
		1.2389	1				
1.192	vw	1.1941	3				

^a JCPDS 22-1036, ^b JCPDS 22-0077

Intensities: s strong; m medium; w weak; v very.

Acknowledgement

Authors are acknowledged to the Ministry of Science and Technology of Slovenia for providing funding. Thanks to Ms. B. Sedej for chemical analyses.

References

- [1] N. Herron, D. L. Thorn, R. L. Harlow, G. A. Jones, J. B. Parise, J. A. Fernandez-Baca, T. Vogt, *Chem. Materials*, **1995**, *7*, 75-83.
- [2] U. Bentrup, *Eur. J. Solid State Inorg. Chem.*, **1992**, *29*, 51-61.
- [3] R. Weinland, I. Lang, A. Fikentscher, *Z. Anorg. Chem.*, **1926**, *50*, 47-54.
- [4] S. Miličev, A. Rahten, *Eur. J. Solid State Inorg. Chem.*, **1991**, *28*, 557-566.
- [5] J. Slivnik, J. Pezdič, B. Sedej, *Monatsh. Chem.*, **1967**, *98*, 200-205.
- [6] Darko Hanžel, A. Rahten, D. Hanžel, *Eur. J. Solid State Inorg. Chem.*, **1994**, *31*, 381-390.
- [7] A. Meden, J. Šiftar, L. Golič, *Acta Cryst.*, **1996**, *C52*, 493-496.
- [8] L. F. Audrieth and B. Ackerson – Ogg, *The Chemistry of Hydrazine*, Wiley, New York, 1951, pp. 48-51.
- [9] P. Glavič, J. Slivnik, *Monatsh. Chem.*, **1967**, *98*, 1878-1880.
- [10] W. R. McBride, R. A. Henry, S. Skolnik, *Anal. Chem.*, **1951**, *23*, 890-893.
- [11] A. I. Vogel "A Textbook of Quantitative Inorganic Analysis", Longmans, London, 1978, pp. 312-314.
- [12] A. K. Covington, *Ion - Selective Electrode Methodology*, CRC Press, Inc., Boca Raton, Florida, 1984, Vol. I, pp. 175-245, and Vol. II, pp. 65-109.
- [13] R. Pribil, *Applied Complexometry*, Pergamon Press, Oxford, England, 1982, 171-178.
- [14] *teXsan for Windows: Crystal Structure Analysis Package*, Molecular Structure Corporation, 1997.
- [15] S. Miličev, J. Maček, *Spectrochim. Acta*, **1985**, *41A*, 651-655.
- [16] P. Bukovec, *Monatsh. Chem.*, **1974**, *105*, 517-524.
- [17] P. Bukovec, B. Orel, J. Šiftar, *Monatsh. Chem.*, **1971**, *102*, 885-895.
- [18] E.J. Baran, A. E. Lavat, *Z. Naturforsch.*, **1981**, *36A*, 677-679.
- [19] M. J. Reissfeld, *Spectrochim. Acta*, **1973**, *29A*, 1923-1926.
- [20] B. Kojić-Prodić, S. Ščavničar, R. Liminga, M. Šljukić, *Acta Cryst.*, **1972**, *B28*, 2028-2032.
- [21] E. C. Hamilton, J. A. Ibers, "Hydrogen Bonding in Solids", W. A. Benjamin, New York, 1968, pp. 15-18.
- [22] M. N. Burnett, C. K. Johnson, ORTEP-III, Report ORNL-6895. Oak Ridge National Laboratory, Oak Ridge, Tennessee, 1996.
- [23] J. Slivnik, J. Maček, A. Rahten, B. Sedej, *Thermochim. Acta*, **1980**, *39*, 21-33.
- [24] U. Bentrup, *Z. anorg. allg. Chem.*, **1993**, *619*, 954-960.
- [25] A. Rahten, S. Miličev, *Thermochim. Acta*, **1997**, *302*, 137-141.
- [26] M. Grobelny, *J. Fluorine Chem.*, **1977**, *9*, 187-207.
- [27] D. H. Mentz, U. Bentrup, *Z. Anorg. Allg. Chem.*, **1989**, *576*, 186-196.

Povzetek

Z reakcijo med $\text{AlF}_3 \cdot 3\text{H}_2\text{O}$ in $\text{N}_2\text{H}_5\text{F}$ v vodni raztopini je bil sintetiziran $(\text{N}_2\text{H}_5)_3\text{AlF}_6$. V infrardečem spektru $(\text{N}_2\text{H}_5)_3\text{AlF}_6$ se pojavi N-N valenčno nihanje N_2H_5^+ iona kot srednje močan trak pri 969 in močan trak pri 955 cm^{-1} , v ramanskem spektru pa pri 965 in 955 cm^{-1} , kar kaže na različno okolje na okolico občutljivega iona N_2H_5^+ . Spojina kristalizira v ortorombski prostorski skupini $\text{P}2_12_12_1$ (št.19) z dimenzijami osnovne celice $a=9.015(2) \text{ \AA}$, $b=9.191(2) \text{ \AA}$ in $c=10.479(2) \text{ \AA}$. Struktura $(\text{N}_2\text{H}_5)_3\text{AlF}_6$ sestoji iz samostojnih oktaedrov AlF_6^{-3} , ki se zlagajo v popačeni ploskovno centrirani kubični sklad in so med sabo povezani preko hidrazinijevih(1+) ionov. Glede na orientacijo $\text{NH}_2\text{-NH}_3^+$ enot obstajata dva tipa močnih vodikovih vezi. Termični razkroj $(\text{N}_2\text{H}_5)_3\text{AlF}_6$ poteče z eksotermnim razkrojem hidrazinijevega iona preko mešanice $(\text{NH}_4)_3\text{AlF}_6$ in NH_4AlF_4 pri 243°C . Pri nadaljnjem razkroju pri 301°C nastane NH_4AlF_4 in pri 460°C $\beta\text{-AlF}_3$. Končni produkt termičnega razkroja pri 700°C je $\alpha\text{-AlF}_3$.